Magnetic Resonance in Medicine 67:251–257 (2012)

In Utero Phenotyping of Mouse Embryonic Vasculature With MRI

Cesar A. Berrios-Otero,[1,2] Brian J. Nieman,[1†] Prodromos Parasoglou,[1] and Daniel H. Turnbull[1–4*]

The vasculature is the earliest developing organ in mammals and its proper formation is critical for embryonic survival. MRI approaches have been used previously to analyze complex three-dimensional vascular patterns and defects in fixed mouse embryos. Extending vascular imaging to an in utero setting with potential for longitudinal studies would enable dynamic analysis of the vasculature in normal and genetically engineered mouse embryos, in vivo. In this study, we employed an in utero MRI approach that corrects for motion, using a combination of interleaved gated acquisition and serial coregistration of rapidly acquired three-dimensional images. We tested the potential of this method by acquiring and analyzing images from wildtype and *Gli2* mutant embryos, demonstrating a number of *Gli2* phenotypes in the brain and cerebral vasculature. These results show that in utero MRI can be used for in vivo phenotype analysis of a variety of mutant mouse embryos. Magn Reson Med 67:251–257, 2012.

Key words: angiogenesis; basilar artery; carotid artery; *Gli2* mutant mice

The mouse is the model organism of choice for studies of mammalian development and human developmental disorders. The ability to create targeted mutations and transgene insertions into the mouse genome has enabled genetic experiments that have provided important insights into the complex processes that take place during mammalian development and disease. Although MRI analyses of postnatal and adult mouse phenotypes is now commonplace, many genetic mutations cause embryonic and early postnatal lethality, limiting phenotype analysis to ex vivo studies in the majority of cases. Of particular interest due to its critical function during embryogenesis is the elucidation of genes involved in vascular development and disease (1). This process results in a complex, three-dimensional (3D) network of vessels that are essential for the transport of oxygen, metabolites, and hormones necessary for growth. Volumetric imaging methods such as MRI can provide powerful and quantitative tools for the analysis of vascular patterning in both normal and mutant mouse embryos (2).

Previous MRI studies of mouse embryonic vasculature have mostly been performed ex vivo on fixed samples, providing high-resolution 3D images (3–8). However, these methods only provide a static view of the vascular system at a particular embryonic stage, limiting our ability to describe the dynamic processes that take place during embryogenesis. For in vivo MRI of vascular development, ferritin-expressing transgenic mice were generated for in utero detection of T_2-weighted signal changes in embryonic vascular endothelial cells (9). While this is potentially a powerful method, high-resolution 3D in utero images of vascular patterns have not been demonstrated, and the approach requires breeding the ferritin-expressing transgenic mice with each mutant mouse line under investigation. A sensitive, high-resolution MRI method for 3D imaging of the embryonic mouse vasculature, based solely on endogenous contrast mechanisms, would provide a more accessible approach for longitudinal in utero studies of vascular development and phenotype analysis in the widest variety of mutant mouse models.

The *Sonic Hedgehog* (*Shh*) signaling pathway is critical for normal mammalian development (10), and recently there has been an increased interest in the role of *Shh* in vascular development (11). However, no detailed analyses have been reported on the roles of the mouse *Gli* genes, the major effectors of *Shh* signaling, particularly during vascular development. We have previously reported an MRI phenotype analysis of $Gli2^{-/-}$ embryos using ex vivo imaging techniques to reveal a severe vascular defect in the posterior brain regions (3).

In this study we used an in utero MRI method that uses self-gated acquisition to select data with minimal motion artifacts. Self-gated acquisition was combined with coregistration and averaging of a series of short acquisition time, low signal-to-noise ratio (SNR) 3D images (12). Embryonic vasculature was detected and visualized using the inherent contrast between blood and surrounding fetal tissues. We tested the potential of this method for developmental and phenotypic analysis by imaging embryonic day (E)17.5 wildtype (WT) and $Gli2^{-/-}$ mutant embryos (13), in utero, and demonstrated the ability to detect both brain and cerebral vascular phenotypes.

[1]The Kimmel Center for Biology and Medicine at the Skirball Institute of Biomolecular Medicine, New York University School of Medicine, New York, New York, USA.
[2]Developmental Genetics Graduate Program, New York University School of Medicine, New York, New York, USA.
[3]Department of Radiology, New York University School of Medicine, New York, New York, USA.
[4]Department of Pathology, New York University School of Medicine, New York, New York, USA.
[†]*Present address:* Mouse Imaging Centre, Hospital for Sick Children, Toronto ON, Canada.
Grant sponsor: NIH; Grant numbers: R01HL078665, R01NS038461.
*Correspondence to: Daniel H. Turnbull, Skirball Institute of Biomolecular Medicine, New York University School of Medicine, 5th Floor, Labs 6-7, 540 First Avenue, New York, NY 10016.
E-mail: Daniel.Turnbull@med.nyu.edu
Received 3 January 2011; revised 22 March 2011; accepted 11 April 2011.
DOI 10.1002/mrm.22991
Published online 16 May 2011 in Wiley Online Library (wileyonlinelibrary.com).

MATERIALS AND METHODS

Animals

All procedures involving mice were approved by the Institutional Animal Care and Use Committee at New York University School of Medicine. WT analysis was initially performed on pregnant Swiss Webster female mice (Taconic). For mutant analysis, *Gli2*$^{+/-}$ heterozygous mutant mice (kindly provided by the Joyner lab) were bred to generate *Gli2*$^{-/-}$ (homozygous mutant), *Gli2*$^{+/-}$, and *Gli2*$^{+/+}$ embryos (grouped together as "wildtype," WT, as no mutant phenotypes have been reported or observed by us in *Gli2*$^{+/-}$ embryos or postnatal mice). All in utero imaging was performed in pregnant mice (6–10 weeks of age), acquiring data from embryos on embryonic day E17.5, where E0.5 was defined as noon of the day after overnight mating. To ensure proper identification of the imaged embryo, either the left or the right uterine horn was imaged in each mouse. The pregnant female was sacrificed immediately postimaging, and the embryo from the imaged side was extracted based on anatomical landmarks from the MRI pilot scans. Polymerase chain reaction of embryonic tissue DNA was used to identify genotypes, using primers for *Neo* and *Gli2*, as previously described (13).

Imaging Methods

Pregnant mice were prepared for imaging in an induction chamber with 4–5% of isoflurane and then transferred to the imaging holder and coil assembly where they were maintained under anesthesia using 1.0–1.5% isoflurane in air supplemented with 30% of oxygen. The murine uterine environment has been reported to be very hypoxic (1–5% oxygen; 14–16), resulting in relatively high levels of deoxygenated fetal blood. Previous reports have estimated that T_2 values can be as low as 4 ms in deoxygenated blood (17,18), with a concomitant much lower expected value for T_2^*. Therefore, we used a 3D gradient echo sequence (echo time = 5.5 ms; repetition time = 17 ms; flip angle = 12°), which resulted in sensitive detection of fetal blood even with a relatively short echo time (5.5 ms). We initiated the study by acquiring 125-μm isotropic resolution images and subsequently implemented an acquisition protocol with variable field of view (min = 24.0 × 13.8 × 9.0 mm^3; max = 24.0 × 18.0 × 9.0 mm^3) and matrix size (min = 208 × 120 × 78; max = 208 × 156 × 78), to accommodate for variable embryo position. This resulted in 115-μm isotropic resolution images acquired in an imaging time of 3.3 min as described previously (12). This scan was repeated serially 50 times for a total acquisition time of 2 h 45 min. The serial scans were combined in reconstruction to obtain a single 3D image. The gradient-echo sequence also incorporated a modified gradient timing—a delay in the phase encode gradients relative to the readout diphase gradient—so that a gating signal could be acquired in every repetition time period for retrospective gating during the image reconstruction (9). All imaging experiments were performed on a 7 T MRI system, consisting of a Biospec Avance II console (Bruker Biospin MRI, Ettigen, Germany) interfaced to a 200-mm horizontal bore superconducting magnet (Magnex Scientific, Yarnton, UK) with an actively shielded gradient coil (BGA9-S; Bruker BioSpin MRI; 90 mm inner diameter, 750 mT/m gradient strength, and 100 μs rise time). Image data were acquired with a custom surface coil (length = 40 mm; width = 16 mm) for receive and a volume resonator (72-mm inner diameter quadrature resonator; Bruker BioSpin MRI) for transmit.

For ex vivo embryo micro-MRI, we used a previously described protocol (3). Briefly, embryos were surgically removed from the uterus maintaining vascular connections to the placenta and warmed at 37°C. Following the perfusion of a phosphate buffered saline/heparin solution and fixation with a 2% (vol/vol) glutaraldehyde/1% formalin solution in phosphate buffered saline, individual embryos were subsequently perfused with a contrast agent (gadolinium - diethylene triamine pentaacetic acid - bovine serum albumin, Gd-DTPA-BSA in gelatin). The umbilical vessels were sutured, and the embryos were immersed in fixative at 4°C to completely fix the embryonic tissues and solidify the gelatin-based contrast agent. Embryos were then imaged using the 7 T MRI system as described above. A quadrature Litz coil (inner diameter = 25 mm, length = 22 mm; Doty Scientific, Columbia, SC) was used to image multiple embryos mounted inside a 30 mL syringe, and imaging was performed using a 3D T_1-weighted gradient echo sequence (echo time = 5 ms; repetition time = 50 ms; flip angle = 35°; field of view = 25.6 mm; matrix size = 512^3; isotropic resolution = 50 μm; total imaging time = 14 h 35 min).

In Vivo Embryonic Image Registration and Reconstruction

For reconstruction of in utero image acquisitions, the series of 50 low SNR embryo images were either averaged directly in *k*-space or registered before averaging to correct embryo positional shifts over the course of the scan as previously described (12). Briefly, six-parameter, rigid body registration was performed using software produced by the Montreal Neurological Institute (http://www.bic.mni.mcgill.ca/ServicesSoftwareAdvancedImageProcessingTools/RegistrationTools) (19). A coarse, manually drawn mask covering the embryonic brain in the initial image was used for registration of each subsequent image acquired during the scan (Fig. 1b). Translation and rotation parameters from the six-parameter transforms were used to compute equivalent *k*-space transformations. Subsequently, the transformed *k*-space lines were averaged together after discarding lines affected by maternal respiration (Fig. 1c). Finally, a histogram-based intensity nonuniformity correction was performed on individual 3D datasets to account for the linear drop of the signal due to the use of a surface receiver coil (20). For vessel visualization (as in Fig. 1d), images were contrast inverted and filtered using a second-order derivative of a gaussian kernel (Fig. 1d). During the registration process, we also obtained data on the (*x*,*y*,*z*) displacements of each image voxel from the initial (reference) image voxel. As a simple measure of the relative motion in each scan, we computed from these data a net magnitude displacement representing the translational displacement of the embryo head from the start to the end of the 2.75-h scan.

Image Analysis

For in vivo data, images were converted into 16-bit and interpolated using a windowed sinc interpolation

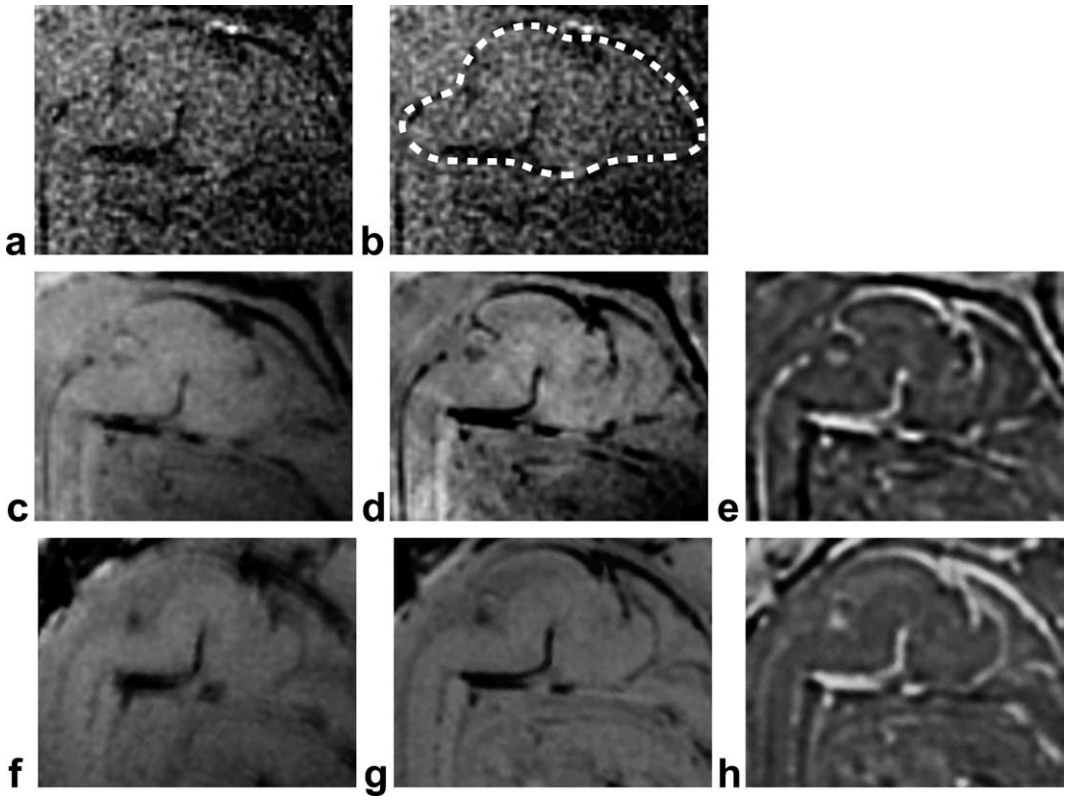

FIG. 1. Image registration and processing methods for visualizing the embryonic vasculature. A series of individual low SNR images were acquired using in vivo imaging methods (**a**) and a mask (dashed outline, panel **b**) was drawn manually around the embryonic brain and blood vessels and used to register the 50 serially acquired low SNR images. Examples are provided of two embryos with different net displacements over the 2.75-h scan, comparing simple *k*-space averaging with registration averaging: embryo 1 (net displacement = 0.5 mm) (**c–e**); embryo 2 (net displacement = 1.0 mm) (**f–h**). Averaging without registration (c,f) produced obviously blurred images with limited (hypointense) vascular detail compared to averaging after registration (d,g), especially in embryo 2 (f,g). Processing of the registered-averaged images with a contrast-inverting filter (e,h) produced improved visualization of the vasculature. (Note: For visualization purposes, cropped midsagittal sections of the 3D images have been presented here.)

function. After processing, individual embryos were manually segmented using a combination of Display (Montreal Neurological Institute) and Analyze (V7.0; AnalyzeDirect, Overland Park, KS). For ex vivo data, multiembryo datasets were converted into 16-bit and interpolated using a windowed sinc interpolation function. Subsequently, images were imported and segmented using Analyze. Individual WT and *Gli2*$^{-/-}$ slices were selected from in vivo image sets and visualized using tricubic interpolation. Three-dimensional visualization of the developing vasculature was achieved by semiautomatic, threshold-based segmentation of the vasculature using Amira (V4.1.1; Visage Imaging, San Diego, CA). We also performed region-of-interest analysis in Analyze to compare signal intensities in selected regions of interest of WT and *Gli2*$^{-/-}$ mouse embryos, using the two-tailed Student's *t*-test to test for statistical significance (set at $P < 0.05$).

RESULTS

In Utero MRI Reveals the Developing Vasculature

In utero MRI was used to locate mouse embryos in the maternal abdomen using pilot scans, and then high-resolution (125- or 115-μm isotropic) images were acquired. Using a 3D gradient echo pulse sequence, the rapidly acquired, low SNR images provided sufficient detail to identify specific regions, including the embryonic mouse brain (Fig. 1a,b). Previously, we showed that embryonic displacement over the course of a long (2–3 h) scan can be a significant factor limiting image quality (12). To further demonstrate this point, and the advantage of the image registration methods, we reconstructed images of E17.5 WT embryos ($N = 6$), comparing direct *k*-space averaging (Fig. 1c,f) or *k*-space averaging after image registration (Fig. 1d,e,g,h). Direct averaging resulted in obvious blurring of fine details in the final images, an effect that increased with increasing embryonic displacement. Registration averaging resulted in significantly improved images with resolution of fine vascular features, even when the net embryonic displacement was close to 1 mm (Fig. 1g,h). A blooming of the T_2^* blood contrast beyond the vascular walls due to susceptibility effects was observed, nonetheless, this method proved to be excellent for revealing cerebral vascular structures, both arterial and venous (Fig. 2; $N = 6$). Analysis of the acquired images revealed the Circle of Willis and other blood vessels, including the vertebral arteries, middle cerebral arteries, internal carotid arteries, superior cerebellar artery, basilar artery, anterior inferior cerebellar

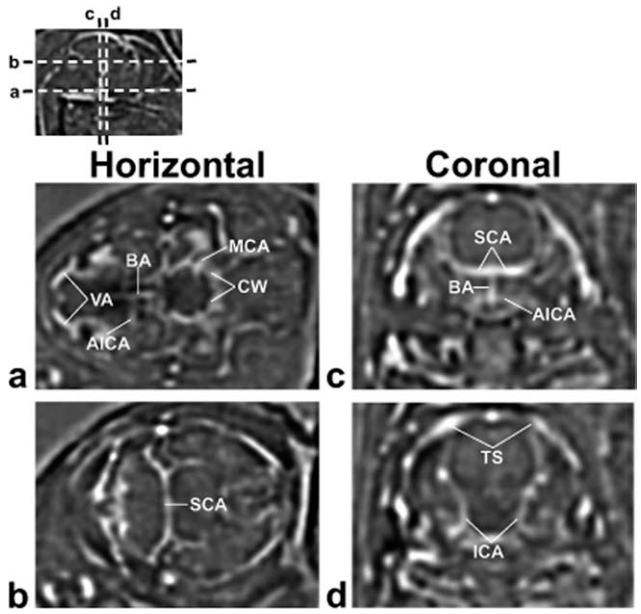

FIG. 2. Two-dimensional sections from in vivo 3D MRI data show the developing vasculature. Horizontal and coronal sections at different levels of the embryonic brain show multiple vessels of the Circle of Willis (CW). Anterior inferior cerebellar artery, AICA; basilar artery, BA; internal carotid arteries, ICA; middle cerebral artery, MCA; superior cerebral artery, SCA; transverse sinus, TS; and vertebral arteries, VA.

arteries as well as the transverse sinuses, the network of veins that surround the brain.

Mutant Phenotypes can be Visualized Using In Utero Micro-MRI

To investigate the potential of this technique for the identification and analysis of developmental phenotypes, we compared 3D, in vivo images acquired from WT ($N = 6$) and *Gli2*$^{-/-}$ ($N = 4$) mutant embryos (Fig. 3). As reported previously from ex vivo data, *Gli2*$^{-/-}$ mutants showed hydrocephaly (enlarged cerebral ventricles), as well as a reduction in size of the midbrain and cerebellum (21–23). Moreover, *Gli2*$^{-/-}$ mutant embryos also showed an alteration of spinal cord shape, in the form of a "kink" in the cervical region that facilitated their identification even on pilot scans (not shown).

Vascular Phenotypes can be Identified and Analyzed Using In Utero Micro-MRI

Analysis of the cerebral vasculature of WT and *Gli2*$^{-/-}$ mutant embryos also revealed a number of vascular phenotypes in the mutant brains (Figs. 4 and 5; $N = 6$, WT; $N = 3$, *Gli2*$^{-/-}$). Most notably, in all *Gli2*$^{-/-}$ mutant embryos, there was an obvious absence of the basilar artery and associated arterial branches, as well as an alteration in the size and geometry of the Circle of Willis evidenced by a reduction in the distance between its component arteries similar to our previous report using ex vivo micro-MRI (3). Signal intensity on the ventral side of the brain, measured in a region-of-interest covering the normal location of the basilar artery, was significantly lower in *Gli2*$^{-/-}$ mutant embryos, confirming the visually described phenotype (mean ± standard deviation: *Gli2*$^{-/-}$ = 1.02 ± 0.03, $N = 3$ vs. WT = 1.35 ± 0.15, $N = 6$; $P < 0.003$). In *Gli2*$^{-/-}$ mutant embryos, we also observed a truncation of the vertebral arteries, which failed to enter the more posterior brain regions, as well as a variable region in the medial-posterior brain, where abnormal vessels occupied part of the space normally occupied by the vertebral and basilar arteries, possibly as a result of abnormal angiogenesis to compensate for the loss of those vessels. Segmentations were also generated, comparing ex vivo contrast-enhanced micro-MRI (Fig. 5a–d) and in utero MRI (Fig. 5e–h) in E17.5 WT (Fig. 5a,b,e,f) and *Gli2*$^{-/-}$ embryos (Fig. 5c,d,g,h). These comparisons demonstrated similar genotype-specific 3D patterns, except in the variable medial-posterior regions of the *Gli2*$^{-/-}$ mutants, after accounting for the inherent difference in resolution (50 μm for ex vivo compared to 115 μm for in vivo) and the blooming of the T_2^* blood contrast beyond the vascular walls.

DISCUSSION

Severe disruptions in numerous organs and vascular networks often result in embryonic and early postnatal

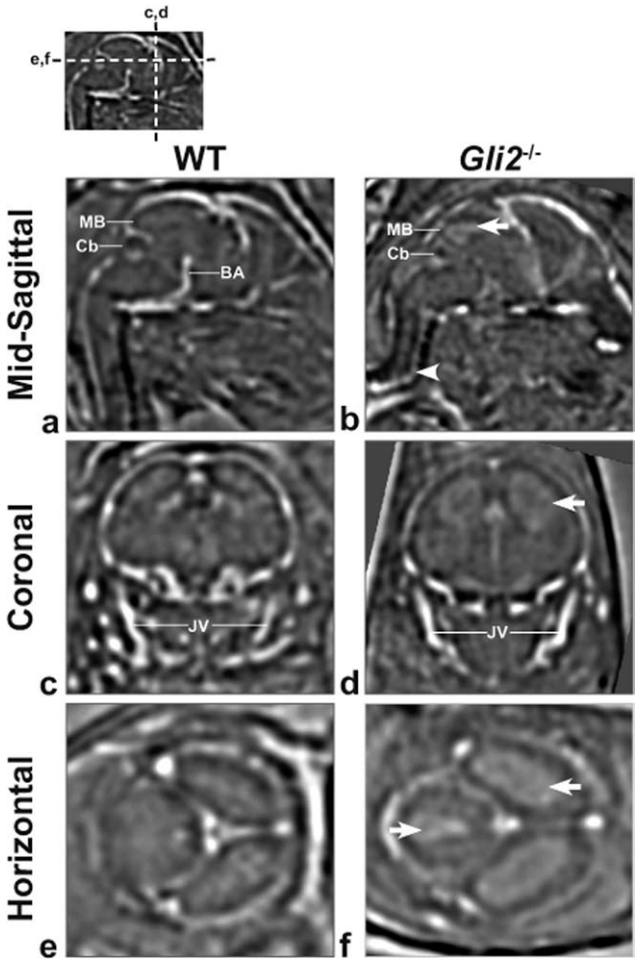

FIG. 3. Central nervous system phenotypes can be visualized using in utero MRI. *Gli2*$^{-/-}$ mutants show multiple nonvascular phenotypes including enlarged ventricles (arrows), abnormal spinal cord patterning (arrowhead), and reduced midbrain (MB) and cerebellum (Cb) size. Basilar artery, BA and jugular vein, JV.

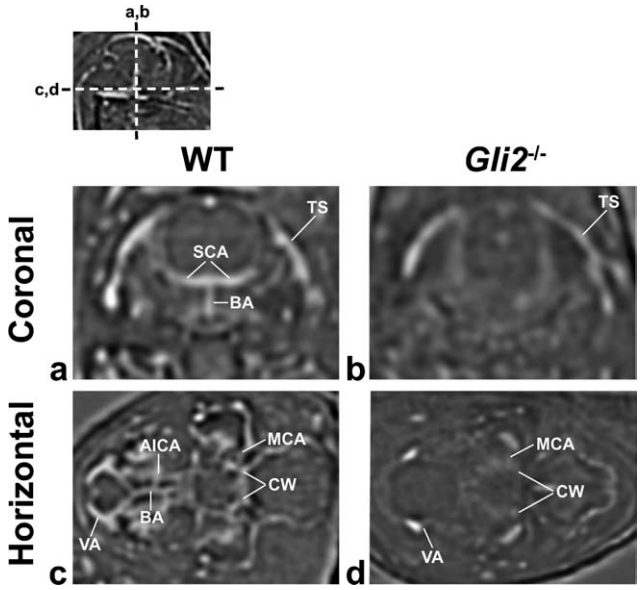

FIG. 4. Multiple vascular phenotypes can be identified in mutant embryos. *Gli2*$^{-/-}$ mutant embryos have a basilar deletion phenotype and vascular patterning defects in blood vessels that compose the Circle of Willis (CW). Anterior inferior cerebellar artery, AICA; basilar artery, BA; middle cerebral artery, MCA; superior cerebral artery, SCA; transverse sinus, TS; and vertebral arteries, VA.

lethality. Previous reports have demonstrated the utility of ex vivo micro-MRI as a tool for analyzing 3D anatomical and vascular defects in fixed mouse embryos (3–8). With the use of self-gating to minimize motion artifacts, combined with image registration methods, we have shown that high resolution, highly detailed data can be acquired in utero from living mouse embryos. Previous reports have shown that some forms of periodic motion, including cardiac and respiratory motion in postnatal animals, can be suppressed with simple *k*-space averaging (24,25). We showed that this strategy is not effective in the face of a permanent displacement, as in fetal imaging, which requires registration before *k*-space averaging (Fig. 1). Using our approach, we demonstrated the in vivo detection and analysis of brain and cerebral vascular phenotypes in *Gli2* mutant embryos. Our results show great potential for in utero 3D MRI to analyze the development of normal vasculature and vascular phenotypes associated with a variety of mutant mouse embryos. This will provide future opportunities for investigating in utero phenotypes lethal in late embryonic or early postnatal stages and should permit longitudinal observation of vascular development in vivo. With the use of higher resolution imaging parameters, combined with closer fitting surface coils and vascular-targeted contrast agents, we anticipate that mouse embryos can be imaged from much earlier stages, enabling longitudinal studies of organ and vascular development.

From a practical point of view, future longitudinal studies will require identification and imaging of an individual mouse embryo from one time point to the next. This challenge is similar for MRI and other in utero imaging modalities such as ultrasound biomicroscopy (26,27). Similar to ultrasound biomicroscopy, careful positioning of the pregnant mouse within the coil and use of the pilot scans to map the fetal positions with respect to adjacent anatomical structures should enable accurate identification of individual embryos over intervals of at least 12–24 h (28). In embryos with clearly defined mutant phenotypes, such as the spinal cord and basilar artery phenotypes in the *Gli2*$^{-/-}$ mice, the mutant

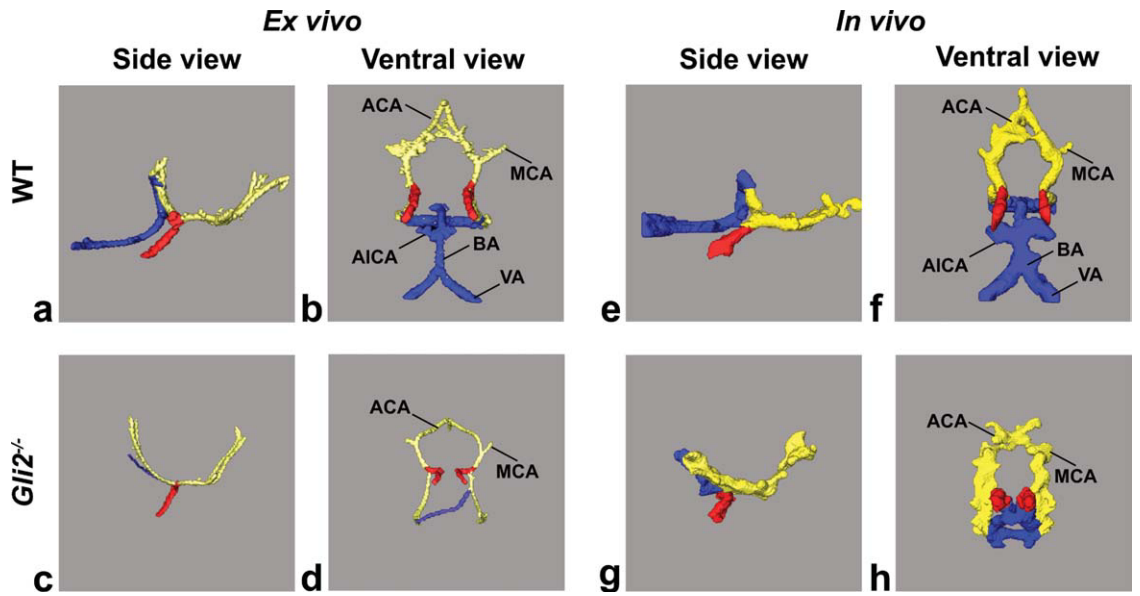

FIG. 5. Three-dimensional volumetric rendering of wildtype and *Gli2* mutant cerebral vasculature in vivo MRI correlates with similar ex vivo renderings. Ex vivo (**a**–**d**) and in vivo (**e**–**h**) 3D rendering views of the Circle of Wills and cerebral vasculature show deletion of the basilar artery and variable alteration of posterior cerebral artery branches (blue), constriction between the left and right carotid arteries (red), and overall geometric differences in the Circle of Willis (yellow) between WT (top row) and *Gli2* mutants (bottom row). Anterior cerebral artery, ACA; anterior inferior cerebellar artery, AICA; basilar artery, BA; middle cerebral artery, MCA; and vertebral arteries, VA.

defects themselves may be useful for identifying individual embryos on subsequent imaging sessions. Ultrasound biomicroscopy is superior to MRI in terms of image acquisition time, offering real time (≥100 images/s) frame rates for 2D image acquisition and 3D acquisition in a few seconds. However, ultrasound biomicroscopy has relatively low tissue penetration compared to MRI, as well as low SNR and tissue contrast, and an inherent speckled intensity pattern, highlighting the clear advantages of MRI for producing the image segmentations and visualizations required for effective 3D analysis of vascular development.

Recently, advances in transgenic mouse technology have resulted in the use of fluorescent proteins to label the vasculature of developing embryos (29–31). Although this approach has provided a successful tool for imaging of vascular development in vivo in lower organisms, such as zebrafish (29,32), optical microscopy in mice requires the removal of embryos from the uterus and their maintenance in culture. Although these approaches provide valuable information at the cellular level, there are limitations of optical imaging in terms of penetration depth and restriction to early stages suitable for embryo culture. Moreover mouse embryos can only be cultured for approximately 24 h, limiting developmental studies to a relatively narrow temporal window compared to those accessible to in utero MRI.

MRI reporter genes have been proposed, most notably ferritin, which may provide advantages for future in utero vascular imaging studies (9). We previously showed that (brain specific) manganese administration combined with (maternal) respiration-gated in utero MRI was useful for the identification of embryonic brain phenotypes in vivo (33). A similar approach may be useful to increase the contrast between the vasculature and surrounding tissues. In addition, intravascular injection of contrast agents targeted to vascular endothelial cells may further improve the sensitivity for detecting and analyzing vasculature. This could provide an important future method for molecular imaging of vascular development in mouse embryos, especially if combined with transgenic mouse technology to control the molecular targets for contrast enhancement. Advances in this direction would allow unprecedented tissue-specific longitudinal imaging studies of cardiovascular development in a truly in situ environment, to further understand the complex and dynamic processes involved in establishing the final 3D patterns of the mammalian vascular system.

REFERENCES

1. Rossant J, Howard L. Signaling pathways in vascular development. Annu Rev Cell Dev Biol 2002;18:541–573.
2. Turnbull DH, Mori S. MRI in mouse developmental biology. NMR Biomed 2007;20:265–274.
3. Berrios-Otero CA, Wadghiri YZ, Nieman BJ, Joyner AL, Turnbull DH. Three-dimensional micro-MRI analysis of cerebral artery development in mouse embryos. Magn Reson Med 2009;62:1431–1439.
4. Huang GY, Wessels A, Smith BR, Linask KK, Ewart JL, Lo CW. Alteration in connexin 43 gap junction gene dosage impairs conotruncal heart development. Dev Biol 1998;198:32–44.
5. Schneider JE, Bamforth SD, Farthing CR, Clarke K, Neubauer S, Bhattacharya S. High-resolution imaging of normal anatomy, and neural and adrenal malformations in mouse embryos using magnetic resonance microscopy. J Anat 2003;202:239–247.
6. Schneider JE, Bose J, Bamforth SD, Gruber AD, Broadbent C, Clarke K, Neubauer S, Lengeling A, Bhattacharya S. Identification of cardiac malformations in mice lacking Ptdsr using a novel high-throughput magnetic resonance imaging technique. BMC Dev Biol 2004;4:16.
7. Smith BR, Johnson GA, Groman EV, Linney E. Magnetic resonance microscopy of mouse embryos. Proc Natl Acad Sci USA 1994;91:3530–3533.
8. Wadghiri YZ, Schneider AE, Gray EN, Aristizabal O, Berrios C, Turnbull DH, Gutstein DE. Contrast-enhanced MRI of right ventricular abnormalities in Cx43 mutant mouse embryos. NMR Biomed 2007;20:366–374.
9. Cohen B, Ziv K, Plaks V, Israely T, Kalchenko V, Harmelin A, Benjamin LE, Neeman M. MRI detection of transcriptional regulation of gene expression in transgenic mice. Nat Med 2007;13:498–503.
10. Fuccillo M, Joyner AL, Fishell G. Morphogen to mitogen: the multiple roles of hegehog signalling in vertebrate neural development. Nat Rev Neurosci 2006; 7:772–783.
11. Nagase T, Nagase M, Machida M, Fujita T. Hedgehog signalling in vascular development. Angiogenesis 2008;11:71–77.
12. Nieman BJ, Szulc KU, Turnbull DH. Three-dimensional, in vivo MRI with self-gating and image coregistration in the mouse. Magn Reson Med 2009;61:1148–1157.
13. Mo R, Freer AM, Zinyk DL, Crackower MA, Michaud J, Heng HH, Chik KW, Shi XM, Tsui LC, Cheng SH, Joyner AL, Hui C. Specific and redundant functions of Gli2 and Gli3 zinc finger genes in skeletal patterning and development. Development 1997;124:113–123.
14. Pringle KG, Kind KL, Thompson JG, Roberts CT. Complex interactions between hypoxia inducible factors, insulin-like growth factor-II and oxygen in early murine trophoblasts. Placenta 2007;28:1147–1157.
15. Okazaki K, Maltepe E. Oxygen, epigenetics and stem cell fate. Regen Med 2006;1:71–83.
16. Lee YM, Jeong CH, Koo SY, Son MJ, Song HS, Bae SK, Raleigh JA, Chung HY, Yoo MA, Kim KW. Determination of hypoxic region by hypoxia marker in developing mouse embryos in vivo: a possible signal for vessel development. Dev Dyn 2001;220:175–186.
17. Ogawa S, Lee TM, Nayak AS, Glynn P. Oxygenation-sensitive contrast in magnetic resonance image of rodent brain at high magnetic fields. Magn Reson Med 1990;14:68–78.
18. Ogawa S, Lee TM. Magnetic resonance imaging of blood vessels at high fields: in vivo and in vitro measurements and image simulation. Magn Reson Med 1990;16:9–18.
19. Collins DL, Neelin P, Peters TM, Evans AC. Automatic 3D intersubject registration of MR volumetric data in standardized Talairach space. J Comput Assist Tomogr 1994;18:192–205.
20. Sled JG, Zijdenbos AP, Evans AC. A nonparametric method for automatic correction of intensity nonuniformity in MRI data. IEEE Trans Med Imaging 1998;17:87–97.
21. Palma V, Ruiz i Altaba A. Hedgehog-GLI signaling regulates the behavior of cells with stem cell properties in the developing neocortex. Development 2004;131:337–345.
22. Corrales JD, Rocco GL, Blaess S, Guo Q, Joyner AL. Spatial pattern of sonic hedgehog signaling through Gli genes during cerebellum development. Development 2004;131:5581–5590.
23. Blaess S, Corrales JD, Joyner AL. Sonic hedgehog regulates Gli activator and repressor functions with spatial and temporal precision in the mid/hindbrain region. Development 2006;133:1799–1809.
24. Beckmann N, Tigani B, Ekatodramis D, Borer R, Mazzoni L, Fozard JR. Pulmonary edema induced by allergen challenge in the rat: noninvasive assessment by magnetic resonance imaging. Magn Reson Med 2001;45:88–95.
25. Ble FX, Cannet C, Zurbruegg S, Karmouty-Quintana H, Bergmann R, Frossard N, Trifilieff A, Beckmann N. Allergen-induced lung inflammation in actively sensitized mice assessed with MR imaging. Radiology 2008;248:834–843.
26. Ji RP, Phoon CK, Aristizabal O, McGrath KE, Palis J, Turnbull DH. Onset of cardiac function during early mouse embryogenesis coincides with entry of primitive erythroblasts into the embryo proper. Circ Res 2003;92:133–135.
27. Phoon CK, Ji RP, Aristizabal O, Worrad DM, Zhou B, Baldwin HS, Turnbull DH. Embryonic heart failure in NFATc1–/– mice: novel mechanistic insights from in utero ultrasound biomicroscopy. Circ Res 2004;95:92–99.
28. Ji RP, Phoon CK. Noninvasive localization of nuclear factor of activated T cells c1–/– mouse embryos by ultrasound biomicroscopy-

Doppler allows genotype–phenotype correlation. J Am Soc Echocardiogr 2005;18:1415–1421.
29. Motoike T, Loughna S, Perens E, Roman BL, Liao W, Chau TC, Richardson CD, Kawate T, Kuno J, Weinstein BM, Stainier DY, Sato TN. Universal GFP reporter for the study of vascular development. Genesis 2000;28:75–81.
30. Fraser ST, Hadjantonakis AK, Sahr KE, Willey S, Kelly OG, Jones EA, Dickinson ME, Baron MH. Using a histone yellow fluorescent protein fusion for tagging and tracking endothelial cells in ES cells and mice. Genesis 2005;42:162–171.
31. Larina IV, Shen W, Kelly OG, Hadjantonakis AK, Baron MH, Dickinson ME. A membrane associated mCherry fluorescent reporter line for studying vascular remodeling and cardiac function during murine embryonic development. Anat Rec (Hoboken) 2009;292:333–341.
32. Lawson ND, Weinstein BM. In vivo imaging of embryonic vascular development using transgenic zebrafish. Dev Biol 2002;248:307–318.
33. Deans AE, Wadghiri YZ, Berrios-Otero CA, Turnbull DH. Mn enhancement and respiratory gating for in utero MRI of the embryonic mouse central nervous system. Magn Reson Med 2008;59: 1320–1328.